

San Jose State University
SJSU ScholarWorks

Master's Theses

Master's Theses and Graduate Research

1995

Real-time fingerprint identification by matched filtering

Panfilo C. Deguzman
San Jose State University

Follow this and additional works at: https://scholarworks.sjsu.edu/etd_theses

Recommended Citation

Deguzman, Panfilo C., "Real-time fingerprint identification by matched filtering" (1995). *Master's Theses*. 987.
DOI: <https://doi.org/10.31979/etd.8tua-gr8h>
https://scholarworks.sjsu.edu/etd_theses/987

This Thesis is brought to you for free and open access by the Master's Theses and Graduate Research at SJSU ScholarWorks. It has been accepted for inclusion in Master's Theses by an authorized administrator of SJSU ScholarWorks. For more information, please contact scholarworks@sjsu.edu.

INFORMATION TO USERS

This manuscript has been reproduced from the microfilm master. UMI films the text directly from the original or copy submitted. Thus, some thesis and dissertation copies are in typewriter face, while others may be from any type of computer printer.

The quality of this reproduction is dependent upon the quality of the copy submitted. Broken or indistinct print, colored or poor quality illustrations and photographs, print bleedthrough, substandard margins, and improper alignment can adversely affect reproduction.

In the unlikely event that the author did not send UMI a complete manuscript and there are missing pages, these will be noted. Also, if unauthorized copyright material had to be removed, a note will indicate the deletion.

Oversize materials (e.g., maps, drawings, charts) are reproduced by sectioning the original, beginning at the upper left-hand corner and continuing from left to right in equal sections with small overlaps. Each original is also photographed in one exposure and is included in reduced form at the back of the book.

Photographs included in the original manuscript have been reproduced xerographically in this copy. Higher quality 6" x 9" black and white photographic prints are available for any photographs or illustrations appearing in this copy for an additional charge. Contact UMI directly to order.

UMI

A Bell & Howell Information Company
300 North Zeeb Road, Ann Arbor, MI 48106-1346 USA
313/761-4700 800/521-0600

**REAL-TIME
FINGERPRINT IDENTIFICATION
BY MATCHED FILTERING**

**A Thesis
Presented to
The Faculty of the Department of Physics
San Jose State University**

**In Partial Fulfillment
of the Requirements for the Degree
Master of Science**

**by
Panfilo C. Deguzman
May 1995**

UMI Number: 1374578

UMI Microform 1374578
Copyright 1995, by UMI Company. All rights reserved.

**This microform edition is protected against unauthorized
copying under Title 17, United States Code.**

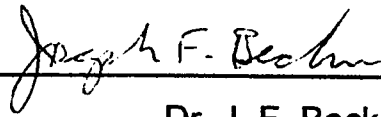
UMI

**300 North Zeeb Road
Ann Arbor, MI 48103**

APPROVED FOR THE DEPARTMENT OF PHYSICS



Dr. R. D. Bahuguna

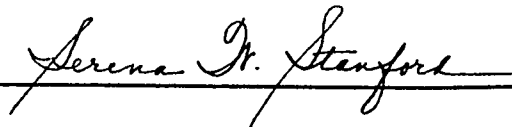


Dr. J. F. Becker



Dr. A. Tucker

APPROVED FOR THE UNIVERSITY



© 1995

Panfilo C. Deguzman

ALL RIGHTS RESERVED

ABSTRACT

REAL-TIME FINGERPRINT IDENTIFICATION BY MATCHED FILTERING

by

Panfilo C. Deguzman

A real-time fingerprint detection system using a matched filter was developed. A fingerprint is extracted using the prism method and recorded with a reference beam to make a hologram. In the setup for character recognition, this hologram is called a matched filter. Results gathered in the development of the real-time system are discussed, as well as results from a detection system made for fingerprint transparencies. The theory of matched filtering and its application to fingerprint identification is presented.

ACKNOWLEDGEMENTS

I would like to thank my thesis advisor, Dr. R. D. Bahuguna, for suggesting this Master's thesis project. In the development of the system, working side by side with him has given me invaluable experience in doing research and development.

I am grateful to HC² Holographic Credit Card for their financial support. I would like to thank Dr. J. Becker and Dr. A. Tucker for reviewing this thesis and for the helpful suggestions they offered. I would also like to thank Retsina Co. for their support, and for giving me access to their machine shop; to SJSU technical staffs Pat Joyce, Minh Mai and Duyen Nguyen for their assistance; and also to Mike Hardy for his work with the different developers and bleaches.

TABLE OF CONTENTS

CHAPTER 1	
Introduction	1
CHAPTER 2	
Fourier transforming properties of lenses	
2.1 Object placed against the lens	3
2.2 Object placed in front of the lens	5
2.3 Object placed behind the lens	6
CHAPTER 3	
Character Recognition using the Vander Lugt filter	
3.1 Synthesis of the Vander Lugt filter	8
3.2 Processing the input data	10
3.3 Application to character recognition	11
CHAPTER 4	
Fingerprint Detection System for Transparencies	
4.1 Basic setup	14
4.2 Noise due to the central order	15
4.3 The transparency effect	16
CHAPTER 5	
Real-Time Fingerprint Detection System	
5.1 Basic recording and detection setups	20
5.2 Magnification of the fingerprint Fourier transform	21
5.3 Optimizing the diffraction efficiency	24
5.4 Extracting a good fingerprint image	25

5.5	Incorporating a laser diode	27
5.6	Construction of the matched filter using glycerol	29
CHAPTER 6		
	Conclusion	30
BIBLIOGRAPHY		31
APPENDIX		32

LIST OF FIGURES

Figure	Title	Page
2.1	Three Fourier transforming configurations.	4
3.1	Illustration of the setup for making a frequency-plane mask for the Vander Lugt filter.	9
3.2	Illustration of the setup for processing input data.	10
3.3	Illustration of the matched filtering operation.	12
4.1	Setup of the fingerprint detection system for transparencies.	15
4.2	Transparency effect observed at the Fourier transform plane due to thickness variations.	17
5.1	Setup for (a) construction and (b) detection of a matched filter.	22
5.2	Illustration of the (a) fingerprint and its (b) Fourier transform.	22
5.3	An illustration of how the prism extracts the fingerprint information.	25

LIST OF TABLES

Table	Title	Page
1	Correlation with the expanded Fourier transform.	18
2	Correlation with the magnified Fourier transform.	19

CHAPTER 1

Introduction

The FBI and other law-enforcement agencies, credit card companies, the welfare and Social Security offices, and private companies concerned with their security system have a strong interest in obtaining an affordable and reliable fingerprint detection system. There are several methods used to design such a system. One method relies on a computer to scan a fingerprint image and compare it with another, one section at a time. Another method uses Fourier Optics, which is the topic of this thesis. It has the advantage of speed in determining true or false recognition. The production of the Fourier transform and matched filtering is essentially done at the speed of light.

In our lab, we have developed a working fingerprint detection system for transparencies where the fingerprint is impressed on a transparency using a photocopier machine. We have further developed a real-time fingerprint detection system where the fingerprint is extracted in real-time by pressing against a prism. In both systems, a coherent laser beam illuminates the fingerprint. The Fourier transform of the fingerprint is produced on a holographic plate placed at the back focal plane of a lens system. An incoming plane wave reference beam interferes with the Fourier transform at the holographic plate and produces a hologram. This hologram, called a matched filter, stores the information of the fingerprint in the form of a Fourier transform. The filter, when illuminated by the original fingerprint beam, will reconstruct the original plane wave reference beam, which is focussed by a lens to a bright spot. The signal of a fingerprint different from the recorded one, however, produces a distorted beam which cannot be made to focus to a bright spot. The intensity of the focussed spot will

then correspond to the degree of correlation and a threshold level can be set to indicate when a match occurs.

CHAPTER 2

Fourier transforming properties of lenses

It is known from diffraction theory¹ that the far field pattern of an object transparency illuminated by a plane wavefront yields a Fourier transform of that transparency along with a phase factor. However, there are two major disadvantages in the spatial Fourier transform for image processing. First, one has to work in the far field region which is not space-efficient. Second, the Fourier transform is associated with a quadratic phase curvature, and therefore we do not obtain an exact Fourier transform at the far field region.

A convex lens basically solves both of these problems. This converging lens has the ability to perform two-dimensional Fourier transformations.² We will consider three Fourier transforming configurations as illustrated in Fig. 2.1. The treatment that follows is from Goodman's book which the reader may refer to for intermediate steps.

2.1 Object placed against the lens

As shown in Fig. 2.1(a), a plane object is placed directly in front of a converging lens having a focal length of f . A monochromatic plane wave with amplitude A illuminates the object which has an amplitude transmittance $t_o(x,y)$. The outgoing signal is given by:

$$U_i(x,y) = At_o(x,y) \quad (2.1)$$

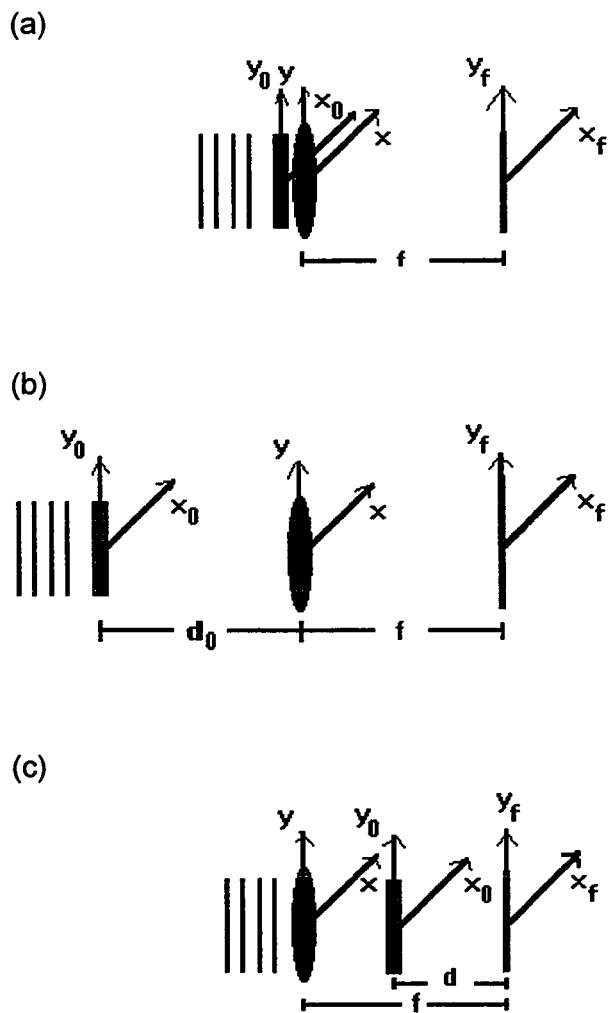


Fig 2.1: Three Fourier transforming configurations. (a) Object placed against the lens (b) Object placed in front of the lens (c) Object placed behind the lens.

After going through the lens, the amplitude distribution becomes:

$$U_l'(x,y) = U_l(x,y) P(x,y) \exp[-j \frac{k}{2f} (x^2+y^2)] \quad (2.2)$$

$$\text{where } P(x,y) = \begin{cases} 1 & \text{inside aperture} \\ 0 & \text{outside} \end{cases}$$

When the object is smaller than the lens, $P = 1$. Using the Fresnel diffraction formula, the amplitude and phase of the light at coordinates (x_f, y_f) at the back focal plane of the lens is given by:

$$U_f(x_f, y_f) = \frac{A \exp[j \frac{k}{2f} (x_f^2 + y_f^2)]}{j\lambda f} \iint t_o(x,y) \exp[-j \frac{2\pi}{\lambda f} (x x_f + y y_f)] dx dy \quad (2.3)$$

A quadratic phase factor appears before the integral; therefore, the relation between the object and the focal-plane amplitude distribution is not an exact Fourier transform.

2.2 Object placed in front of the lens

As shown in Fig 2.1(b), an object transparency is located a distance d_o in front of the lens. A plane wave of amplitude A illuminates the transparency which has the amplitude transmittance represented by t_o . Let $F_o(f_x, f_y)$ represent the Fourier spectrum of light transmitted by the object and $F_L(f_x, f_y)$ represent the Fourier spectrum of light incident on the lens, or equivalently,

$$F_0(f_x, f_y) = \mathcal{F}(A t_0) \quad \text{and} \quad F_L(f_x, f_y) = \mathcal{F}(U_i) \quad (2.4)$$

Using Fresnel approximations for the distance d_0 , we have the relation:

$$F_L(f_x, f_y) = F_0(f_x, f_y) \exp[-j\pi d_0(f_x^2 + f_y^2)] \quad (2.5)$$

The field at the back focal plane of the lens is then given by:

$$U_f(x_f, y_f) = \frac{A \exp\left[j \frac{k}{2f} (1 - d_0/f) (x_f^2 + y_f^2)\right]}{j\lambda f} \cdot \iint t_0(x_0, y_0) \exp\left[-j \frac{2\pi}{\lambda f} (x_0 x_f + y_0 y_f)\right] dx_0 dy_0 \quad (2.6)$$

Note that an exact Fourier transform relation is obtained if the object is placed at the front focal plane of the lens (i.e., $d_0 = f$), which is the condition where the phase curvature vanishes.

2.3 Object placed behind the lens

The amplitude of the spherical wave illuminating the object is Af/d . The object transmits a field amplitude given by:

$$U_f(x_f, y_f) = \frac{A \frac{f}{d} \exp\left[j \frac{k}{2d} (x_f^2 + y_f^2)\right]}{j\lambda f} \cdot \iint t_0(x_0, y_0) \exp\left[-j \frac{2\pi}{\lambda d} (x_0 x_f + y_0 y_f)\right] dx_0 dy_0 \quad (2.7)$$

This is essentially the same as the case with the object placed directly against the lens. The difference is the added flexibility of scaling the Fourier transform by changing the parameter d .

Before concluding this chapter, I would like to point out that a single spherical lens produces a lot of aberration. Therefore, we used lenses that are either doublets or triplets to reduce aberration.

CHAPTER 3

Character Recognition using the Vander Lugt filter

In 1963, A. B. Vander Lugt presented a new technique for synthesizing frequency-plane masks for coherent processors.^{3,4} From patterns of absorption, these masks can control both the amplitude and phase of the transfer function. The Vander Lugt filter has two advantages over the conventional coherent processors:

a. Given an impulse response, the required transfer function is optically synthesized by the system, and thereby eliminates the mathematical calculations of Fourier transforming the impulse response and

b. One absorbing mask is synthesized which has a complicated complex-valued transfer function; it is no longer a complicated task to control the phase transmittance at the frequency plane.

The flexibility of this technique in synthesizing frequency-plane masks has brought about a promising application, such as character recognition.

3.1 Synthesis of the Vander Lugt filter

The frequency-plane mask for the Vander Lugt filter is made using an interferometric system shown in Fig. 3.1.

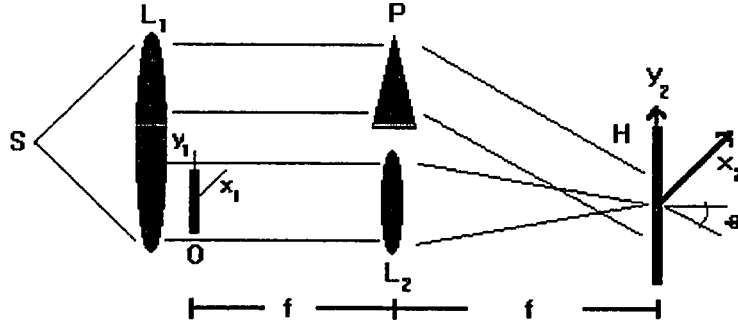


Fig. 3.1: Illustration of the setup for making a frequency-plane mask for the Vander Lugt filter.

The beam from point source S is collimated by lens L₁. A portion of the beam passes through the mask O, and the outgoing signal has an amplitude transmittance equal to the desired impulse response h. The lens L₂ Fourier

transforms the amplitude distribution h to an amplitude distribution $(\frac{1}{\lambda f})$

$H(\frac{x_2}{\lambda f}, \frac{y_2}{\lambda f})$ which then illuminates the holographic film. Another portion of the

collimated beam gets redirected by prism P and strikes the film at angle θ . This tilted plane wave beam is given by:

$$U_r(x_2, y_2) = r_0 \exp(-j2\pi\alpha y_2) , \quad \text{where } \alpha = \frac{\sin\theta}{\lambda} \quad (3.1)$$

The total intensity at the plane of the holographic plate is given by the interference of the two amplitude distributions:

$$I(x_2, y_2) = \left| r_0 \exp(-j2\pi\alpha y_2) + \left(\frac{1}{\lambda f}\right) H\left(\frac{x_2}{\lambda f}, \frac{y_2}{\lambda f}\right) \right|^2 \quad (3.2)$$

$$= r_0^2 + \left(\frac{1}{\lambda f}\right)^2 |H|^2 + r_0 \left(\frac{1}{\lambda f}\right) H \exp(j2\pi\alpha y_2) + r_0 \left(\frac{1}{\lambda f}\right) H^* \exp(-j2\pi\alpha y_2) \quad (3.3)$$

The final step in making the frequency plane mask is the development of the exposed film. This produces a transparency whose amplitude transmittance is proportional to the intensity distribution incident during the exposure:

$$t(x_2, y_2) \propto r_0^2 + \left(\frac{1}{\lambda f}\right)^2 |H|^2 + r_0 \left(\frac{1}{\lambda f}\right) H \exp(j2\pi\alpha y_2) + r_0 \left(\frac{1}{\lambda f}\right) H^* \exp(-j2\pi\alpha y_2) \quad (3.4)$$

3.2 Processing the input data

This filter can now be used to process input data as in the sample system shown in Fig. 3.2.

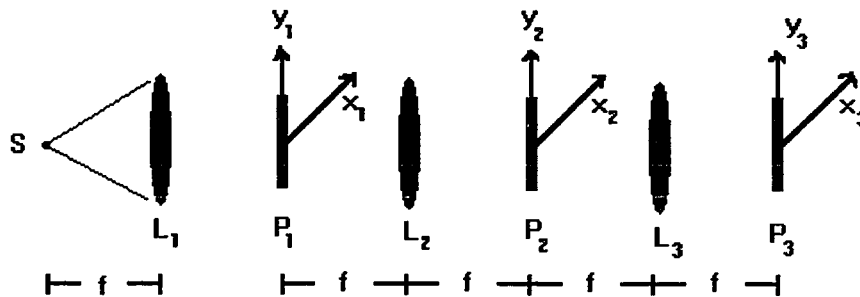


Fig. 3.2: Illustration of the setup for processing input data.

The input function to be filtered is $g(x_1, y_1)$. After the Fourier transformation at lens L_2 , an amplitude distribution $\left(\frac{1}{\lambda f}\right)G\left(\frac{x_2}{\lambda f}, \frac{y_2}{\lambda f}\right)$ would be incident on the frequency-plane mask and the transmitted field would be given by:

$$U_2(x_2, y_2) \propto \left(\frac{1}{\lambda f}\right) r_0^2 G + \left(\frac{1}{\lambda f}\right)^3 |H|^2 G + r_0 \left(\frac{1}{\lambda f}\right)^2 H G \exp(j2\pi\alpha y_2) + r_0 \left(\frac{1}{\lambda f}\right)^2 H^* G \exp(-j2\pi\alpha y_2) \quad (3.5)$$

The final lens L3 Fourier transforms U2 to give:

$$U_3(x_3, y_3) \propto r_0^2 g(x_3, y_3) + \left(\frac{1}{\lambda f}\right)^2 [h(x_3, y_3) * h^*(-x_3, -y_3) * g(x_3, y_3)] + r_0 \left(\frac{1}{\lambda f}\right) [h(x_3, y_3) * g(x_3, y_3) * \delta(x_3, y_3 + \alpha\lambda f)] + r_0 \left(\frac{1}{\lambda f}\right) [h^*(-x_3, -y_3) * g(x_3, y_3) * \delta(x_3, y_3 - \alpha\lambda f)] \quad (3.6)$$

The first and second terms are centered at the origin of the (x_3, y_3) plane, and is not useful for our purpose. The third term written in short-hand notation for convolution can be expanded out into:

$$h(x_3, y_3) * g(x_3, y_3) * \delta(x_3, y_3 + \alpha\lambda f) = \iint h(x_3 - \xi, y_3 + \alpha\lambda f - \eta) g(\xi, \eta) d\xi d\eta \quad (3.7)$$

The fourth term yields the crosscorrelation of g and h and this can be written as:

$$h^*(-x_3, -y_3) * g(x_3, y_3) * \delta(x_3, y_3 - \alpha\lambda f) = \iint g(\xi, \eta) h^*(\xi - x_3, \eta - y_3 + \alpha\lambda f) d\xi d\eta \quad (3.8)$$

The variable α , which varies according to the angle of the reference beam, determines how much the convolution and crosscorrelation will be deflected (in opposite directions) from the axis. The convolution is centered about coordinates $(0, -\alpha\lambda f)$. The crosscorrelation is centered about $(0, \alpha\lambda f)$.

3.3 Application to character recognition

An application of the Vander Lugt filter in character recognition uses the method of match filtering. A filter is matched to the particular signal $s(x,y)$ if its impulse response is given by

$$h(x,y) = s^*(-x,-y) \quad (3.9)$$

An input $g(x,y)$ applied to a filter matched to $s(x,y)$ will produce the cross-correlation function of g and s . This output $v(x,y)$ is given by

$$v(x,y) = \iint h(x-\xi,y-\eta) g(\xi,\eta) d\xi d\eta \quad (3.10)$$

$$= \iint g(\xi,\eta) s^*(\xi-x,\eta-y) d\xi d\eta \quad (3.11)$$

This matched filtering operation is illustrated below in Fig. 3.3:

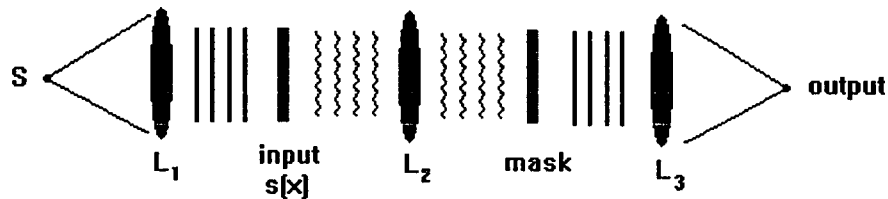


Fig. 3.3: Illustration of the matched filtering operation.

A filter is made by means of a frequency-plane mask in the usual coherent processing setup. It is matched to the input signal $s(x,y)$ and hence have a transfer function $H(f_x,f_y) = S^*(f_x,f_y)$. Thus the frequency-plane mask should have an amplitude transmittance proportional to S^* . Consider now using the original signal s (to which the filter is matched) as the input signal. The mask then

receives a field distribution proportional to S , and transmits a field distribution proportional to SS^* . This quantity has lost the phase factor and is entirely real. The frequency plane mask has canceled all the curvature of the incident wavefront S thereby transmitting a plane wave. Another lens will bring this wave to a bright focus. If an input signal is not $s(x,y)$, the wavefront curvature will in general not be canceled by the frequency-plane mask, and the transmitted light will not be brought to a bright focus by the final lens. Thus we can detect the presence of the original signal $s(x,y)$ by measuring the intensity of the focused light.

CHAPTER 4

Fingerprint Detection System for Transparencies

The goal of the project is to develop a real-time fingerprint detection system. However, we decided that it would be wiser to work with transparencies first and then use our results and experience to guide us through the real-time system. The main advantage of using a transparency over the real-time extraction of the fingerprint from the thumb is that the transparency provides a static fingerprint that has good contrast. The real-time fingerprint can be smudged with oil and sweat of the thumb, and its pattern fluctuates depending on the amount of pressure one uses when pressing against the prism. With the above simplifications, we began by preparing fingerprints using an ink and pad set. Afterwards, we photocopied these fingerprints onto a transparency.

4.1 The basic setup

A setup* of the fingerprint detection system for transparencies is illustrated in Fig. 4.1. A He-Ne laser beam passes through shutter S and beamsplitter BS, dividing the beam into the object and reference beams. The object beam is expanded by microscope objective O and filtered by pinhole PH and is then collimated by lens L_1 . The plane wave beam from L_1 passes through the object transparency T and gets Fourier transformed by lens L_2 at the back focal plane where a holographic plate is placed. The reference beam is directed by mirrors M, expanded and filtered, and then collimated by lens L_3 . This plane wave beam

* Component details are given in the Appendix.

then illuminates the holographic film. A hologram is then made from the interference of the object and reference beams. During detection, the reference beam is unused, and an additional lens L_4 is used to focus the diffracted beam on a detector D .

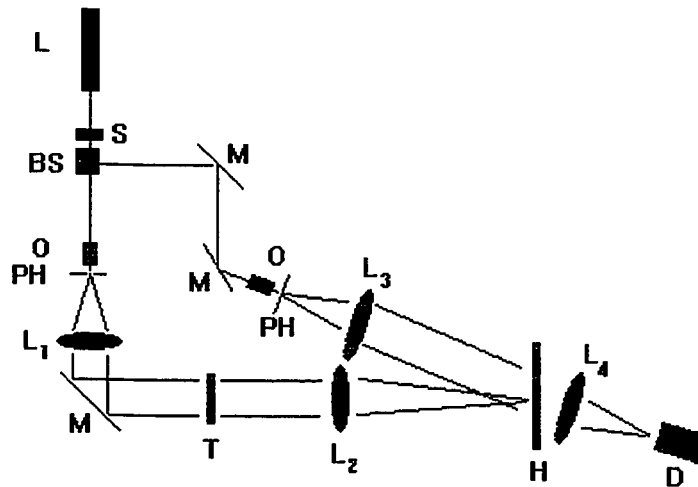


Fig. 4.1: Setup of the fingerprint detection system for transparencies.

4.2 Noise due to the central order

A problem of the fingerprint matched filter is the high noise contribution from the central order. We minimized this problem by overexposing the central order with a focused beam (i.e., we illuminated the plate without the object transparency and without the reference beam). This had the effect of making the central order inactive in the holographic process. Previously, the signal to noise (S/N) ratio was approximately 4 to 1. The removal of the

central order increased the S/N ratio to over 30 to 1. The overexposure of the central portion however resulted in some loss in the correlation signal.

One method of improving the correlation signal was to increase the separation of the important fingerprint signal from the central order. We accomplished this by expanding the Fourier transform ring using a photocopy machine to reduce the fingerprint size. From the natural size of the fingerprint, the spatial frequency comes to about 2 to 10 lines/mm. Reducing the pattern by 64% will have an inverse affect on the spatial frequency, hence the Fourier transform ring expands and now has a larger radius. Because of this additional distance from the center, over-exposing the central region to improve the S/N ratio has less effect on the fingerprint signal than before. A better correlation was consequently achieved.

We tried another method of removing the central order contribution: using a mask similar to what Caulfield and Perkins⁶ used in their system. By adding a microscope objective at the back focal plane of the lens (that Fourier transforms the object transparency signal), the structure was magnified to a manageable size so that an opaque mask could be positioned at the center. More details of this mask is given in the real-time system.

4.3 The transparency effect

The disadvantage of using a transparency is largely from the phase variations introduced by the plastic film. In the manufacturing process of the film, a certain thickness variation is left on the film which acts to introduce phase variations to the incoming beam. The two transparencies we used produced the following distinct patterns at the Fourier transform plane:

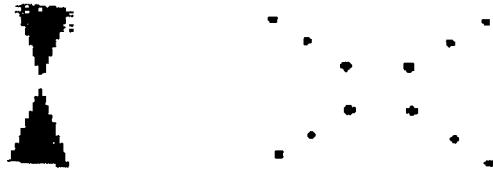


Fig. 4.2: Transparency effect observed at the Fourier transform plane due to thickness variations.

In the process of constructing a matched filter, both Fourier transform signals of the fingerprint and the transparencies are recorded. Hence, not only must the fingerprints match, but so must the transparency signal and orientation. Since several copies of the fingerprints are made on different transparencies and the fingerprints are not exactly oriented in the same manner with respect to the transparency patterns, a high correlation occurs when the recorded setting is duplicated. For example, the cone diffracted by the transparency (as illustrated above) was recorded in the hologram along with the fingerprint signal; thus, correlation partly resulted when transparency cones match. What we wanted was for correlation to occur only when fingerprints match.

To minimize the transparency effect, the Fourier transform signal was adjusted such that it can be separated from the transparency pattern. The cone signal cut through the ring-like structure of the fingerprint Fourier transform; hence, it was difficult to filter it completely. However, the transparency producing the diagonal dots pattern proved more manageable. By reducing the size of the ring such that it was within the diagonal dots, we were able to block the dots using an iris. This reduction in the frequency plane corresponds to a magnification in the spatial plane and this was accomplished by enlarging the normal fingerprint image 120% with a photocopying machine. The spatial

frequency of the fingerprint was then reduced and the corresponding frequency plane pattern was a ring-like structure smaller than before. A number of transparencies were tested and most of the fingerprint copies correlated well. Copies of a different fingerprint likewise did not correlate. One must be careful to avoid touching the transparencies with the fingers since oil from the fingers can easily transfer to the film and introduce more phase variations. The correlations between a recorded fingerprint A, its copies and another different fingerprint B are listed in Table 1 for an expanded Fourier transform and Table 2 for a magnified Fourier transform. The holograms were made using a thermoplastic system.

Once we established the ability of the matched filter to recognize and discriminate the recorded fingerprint pattern from a different one, we moved on to the real-time fingerprint detection system.

Table 1: Correlation with expanded Fourier transform

20 sec over-exposed central spot
 10 ms exposure time
 40% image reduction
 Original print: A
 1 unit = 50 mV on the oscilloscope

Correlation of A with its own copies and with B.

	A	B
Original	5.0 units	
Copy	5.0	0.9
Copy	6.0	0.5
Copy	5.0	0.5
Copy	5.0	0.6
Copy	4.0	0.6
Copy	4.8	0.4
Copy	4.7	0.6

Copy	5.7	0.8
Copy	5.6	0.8
Copy	7.4	
Copy	7.0	
Copy	5.0	
Copy	5.0	
Copy	6.4	
Copy	5.1	
Copy	6.2	
Copy	6.0	

Table 2: Correlation with magnified Fourier transform

10 ms exposure time
 100% image
 Original print: A
 1 unit = 100 mV on the oscilloscope

Correlation of A with its own copies

Original	5.0
Copy	4.8
Copy	4.7
Copy	3.9
Copy	6.0
Copy	6.0
Copy	6.2
Copy	3.6
Copy	6.1
Copy	4.1
Copy	6.4
Copy	3.5
Copy	5.0
Copy	5.9
Copy	5.0
Copy	3.9
Copy	3.2
Copy	6.0
Copy	6.5
Copy	5.0
Copy	4.4

CHAPTER 5

A Real-Time Fingerprint Detection System

We have constructed a real-time fingerprint detection system using the method of matched filtering. Several problems had to be resolved in order to make the system identify fingerprints reliably. We needed to obtain a good fingerprint image, achieve high diffraction efficiency, be able to align the hologram and adjust the optical elements with precision. Further, a miniature system requires good stability, good collimation with short focal-length lenses, and a laser diode to replace the He-Ne laser. This chapter describes in detail the problems involved with developing a real-time fingerprint detection system, as well as the particular solutions we implemented in dealing with them.

5.1 Basic recording and detection setups

The setup** for constructing a matched filter in the real-time fingerprint system is illustrated in Fig. 5.1(a). A beam from a He-Ne laser(L) passes through a shutter(S) and is divided by the beamsplitter(BS) into two beams. Both of the raw laser beams go through a microscope objective(O_1 and O_2) and a pinhole(PH) to produce clean, expanded beams. (Note that one of the beams is guided by mirrors M_1 and M_2 to get to the objective and pinhole.) The beams are then collimated by lenses L_1 and L_3 to produce plane waves. One collimated beam is used as the reference beam and it strikes the holographic plate H. The other collimated beam, used as the object beam, illuminates the surface of the

** Component details are given in the Appendix.

prism (where the thumb presses) and extracts the fingerprint as it leaves the prism. This signal is Fourier transformed by another lens L_2 at its back focal plane. The microscope objective O_3 magnifies the Fourier transform and images it on the holographic plate. Interference occurs between the two beams and a hologram is recorded at the plate.

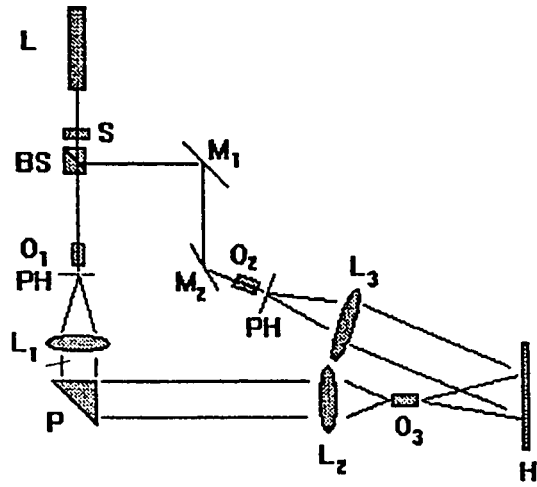
The reconstruction setup is similar to the construction setup except that the reference beam is unused, and an additional lens L_4 is used to focus the diffracted beam on a detector D . This detection setup is given in Fig. 5.1(b).

In the miniaturized version, a laser diode replaces the He-Ne laser (along with the the microscope objective and pinhole) during detection. However, during recording, replacement is not so easy. The coherence length of the laser diode is listed to be in the order of a fraction of a millimeter. In comparison, the He-Ne laser has several centimeters of coherence length. Since recording a hologram requires the path difference between the reference and object beams to be less than the coherence length, recording is more difficult when a laser diode is used. We are currently exploring the possibility of recording a hologram with a laser diode.

5.2 Magnification of the fingerprint Fourier transform

The Fourier transform of the fingerprint recorded at the holographic plate appears as a ring-like structure. A fingerprint and its Fourier transform are shown in Fig. 5.2. In the frequency plane, higher frequency components have larger radii than the lower frequency components. (The zero order is located at the center of the ring.)

(a)



(b)

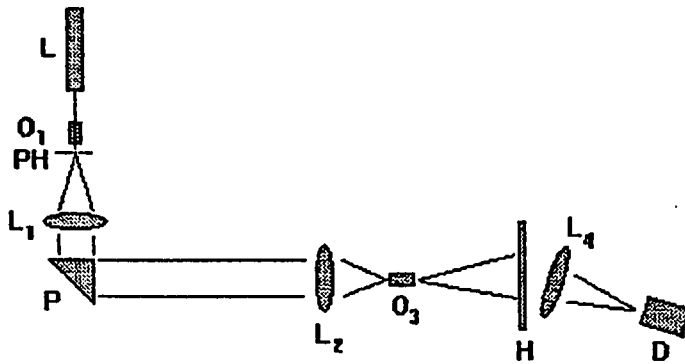


Fig. 5.1: Setup for (a) construction and (b) detection of a matched filter.



(a)



(b)

Fig. 5.2: Illustration of the (a) fingerprint and its (b) Fourier transform.

We had two reasons for magnifying this structure with the microscope objective. First, positioning the hologram was difficult. The size of the ring-like structure is quite small, and is dependent on the focal length of the Fourier transforming lens. The longer the focal length, the bigger the transform ring size. Because we are trying for a very compact apparatus, we are limited to short focal lengths of several inches. This results in a ring structure so minute as to be unrecognizable to the naked eye. Aligning such a structure is therefore difficult during the identification process. With the magnification, the size can be adjusted to whatever is suitable. The alignment is aided by the highly intense zero order component striking the middle of the ring. Even after bleaching, this central spot is still visibly dark and therefore works perfectly as an alignment spot. Once the hologram is centered, it is then rotated to the position ⁵ (within $\pm 1^\circ$) which gives the maximum correlation peak.

The second reason for enlarging the Fourier transform ring is to remove the intense zero order frequency which is common to all fingerprints. It appears to come from factors such as the skin surface area in contact with the input prism. But blocking the central order is practically impossible to do on an unmagnified ring structure that is extremely small. With the enlarged image, a mask can be easily placed at the ring center to block this low frequency signal while allowing the high frequency concentric bands to pass through. Information contained in these bands relate primarily to the fingerprint pattern and other patterns such as pores, ridge details and scars. By passing only the information which is unique to the fingerprint, a better discrimination is achieved.

5.3 Optimizing the diffraction efficiency

Since recognition is principally done by a matched filter, which is a hologram, much effort was spent in finding the optimum conditions for obtaining the best diffraction efficiency. It was apparent at the initial stages of the development of the system that discrimination critically depended on the quality of the hologram, to the point where discrimination is totally lost when the diffraction efficiency is low. Several developers and bleaches were tried. The development and bleaching times were also investigated to obtain best results. It was also important to determine the best object-to-reference beam ratios.

Developers like D19, Pyrogallol and Pyrocatechol were tried. Cathechol gave us the best results by developing for approximately one minute, while adjusting the exposure time to have the plate darken to an optical density of 2. The required exposure time was found to be around 300ms. The bleaches we tried were the dichromate bleach and amidol. Amidol worked best with Cathechol despite its deceptively dark color. A period of one minute was sufficient for bleaching the holographic plate developed to an optical density of 2. A much longer time period would suggest that the plate had been over-developed or over-exposed.

An appropriate object-to-reference beam intensity ratio can be obtained by observing the Fourier transform ring structure and the reference beam at the holographic plate. The ring should be just visible from the uniform background of the reference beam. This situation gave us, so far, the best diffraction efficiency. We have reached diffraction efficiencies up to 26%; the theoretical maximum of phase holograms is 33%.

5.4 Extracting a good fingerprint image

An important matter to consider for a reliable detection is the mechanism for extracting the fingerprint pattern. As shown in Fig. 5.3, the thumb surface is made up of valleys and ridges (exaggerated).

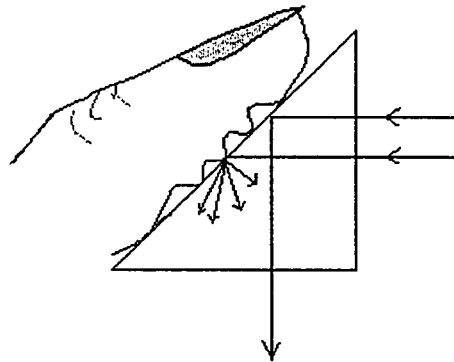


Fig. 5.3: An illustration of how the prism extracts the fingerprint information.

When a laser beam enters the glass prism ($n=1.5$) normally on the vertical surface, it experiences total internal reflection at the diagonal surface (where the thumb is located) since it strikes this surface at an angle of 45° , a value larger than the critical angle. However, when the thumb presses on the surface, the total internal reflection is disrupted at certain regions. When the beam strikes the surface where a valley of the thumb is located, total internal reflection is unaffected, and bright bands tracing the valleys are produced. However, when the beam strikes the surface where a ridge is located, this beam penetrates through the prism and into the finger where it is then scattered in all directions. This frustration of the total internal reflection produces the dark bands tracing the ridges. The key to getting a fingerprint image with good contrast is therefore to

have good contact between the ridges of the thumb and the prism, and to have no contact between the valleys and the prism.

Different conditions of the thumb cause different problems in making an identification. An overly dry thumb lacks good contact with the prism and will produce an image with terrible contrast. Meanwhile, sweaty or oily thumbs usually produce a much better contrast, except when there is too much sweat or oil and the image gets smudged. The ability of the matched filter to recognize a match depends on the quality of the incoming image. A dry thumb, despite being matched to the hologram, could produce a low correlation signal, whereas an unmatched thumb, with the right amount of moisture, may give a large correlation signal just by sending a good image.

We searched for ways to regulate the dry and wet conditions of the thumb. We found several ways to do this. For example, a very reliable but commercially impractical means is to cover the thumb with black ink. The ink covers the pores of the skin to prevent sweat or oil from smudging the fingerprint. It also has a sticky feel to it and this allows for a better contact with the prism, hence solving the problem faced by dry thumbs. Since the ink is black, there is more absorption at the ridges and the contrast is further improved.

The black ink has given us a reliable means of obtaining the proper discrimination of fingerprint signals. Usually when the medium used is wet, like glycerol, thin oil, or water, a spurious signal due to the liquid is incorporated into the correlation signal. This signal arises from random scattering of the laser beam after striking the liquid surface which has height variations. In fact, this spurious signal is observed each time the prism is cleaned with isopropyl alcohol. As the prism surface gets wet, the laser beam is scattered and reflected at random angles and the hologram will receive enough portion of this beam such as to falsely trigger an identification. This is a legitimate concern to us

since an unattended apparatus can be falsely triggered by anyone spraying the prism surface with isopropyl alcohol or any suitable liquid.

A discrimination test between the original fingerprint and a differing one (both coated with black ink) consistently gave a discrimination ratio of 7 to 5. Despite the reliability, however, it is impractical to have users ink their thumbs each time they use the system.

A more practical but less reliable solution is to use a gel, such as hair gel which is rather smooth and thin when applied to the thumb, but becomes dry and sticky a few seconds later. When a thumb which has a large quantity of gel is first pressed on the prism surface, the fingerprint valleys and ridges are smudged by the creamy nature of the gel and gives a false spike weaker in comparison to other liquids. Besides the problem with the initial spike, the gel also dries too much and too quickly than desired, therefore frequent reapplication is necessary in order to achieve a consistent correlation value.

Other media we used were glue stick, Elmer's glue, and spray adhesive. The advantage of using these media are that they are practically dry and very sticky when applied to the finger. There is no signal spike at the initial press of the thumb as present in liquid/gel mediums and they also stay sticky for quite a long period. The only drawback with the glue stick occurs during the application when it tends to be thick and difficult to apply uniformly over the thumb. We are still determining the effectiveness of the Elmer's glue and spray adhesive.

5.5 Incorporating a laser diode

There were several problems brought about by incorporating a 5mW laser diode having 670 nm wavelength into the system. Firstly, the dimension of the diode is about 5 by 70 microns, thus the lateral size of 70 microns can hardly be considered a good point source. In fact, when we attempted to focus a plane wave at the back focal plane of the Fourier transforming lens, the spot did not focus well. Therefore, the problem of spatial coherence emerged. We improved the spatial coherence by increasing the distance of the laser diode source from the collimating lens. Initially, we were using a 3 inch focal length lens and eventually increased it to a 16 inch focal length lens with a noticeable improvement in collimation.

A second problem simultaneously solved by increasing the distance of the laser diode was the expansion of the beam and the consequent uniformity of the beam. The diode beam is made up of vertical bands, the center being the most intense. When the diode is not given enough distance, the beam becomes non-uniform, therefore the fingerprint pattern gets unequal distribution throughout the total area. When the thumb is not placed at the same position in which it was recorded, for example, assume it is no longer at the center where the maximum intensity is located, then the correlation signal decreases because of the lower intensity illuminating that region. By sufficient expansion, uniformity was achieved and slight lateral shifts of the thumb hardly decreases the signal strength.

Another slight problem introduced by the diode was its 670 nm wavelength, as compared to the 632.8 nm wavelength of the He-Ne laser which constructed the hologram. The larger wavelength magnified the Fourier transform structure by the factor of 6%; therefore, we compensated for this

magnification by reducing the distance of the holographic plate from the microscope objective, thereby decreasing the size to approximately that of the original one.

5.6 Construction of the matched filter using glycerol

One of the methods we used in making the matched filter is to use glycerol as the input medium. The thumb is coated lightly with glycerol. Then, it is pressed on the prism and released. An image with good contrast is left on the prism surface and a hologram is made. The advantage of this method is that the fingerprint is static, similar to the hologram of a transparency; hence, there is no problem of excessive body motion while recording. The other advantage is the excellent contrast given by glycerol when the correct amount is used.

CHAPTER 6

Conclusion

A working fingerprint detection system done in real-time has been developed using a matched filter. Although it is not yet in a commercial stage, there are plenty of good reasons to feel optimistic about its future. It gives consistent discrimination of the recorded fingerprint from differing ones. Several important factors have been discussed such as the necessity of obtaining an image with good contrast at the prism, the construction of high diffraction efficiency holograms, and the adjustments required to reconstruct with a laser diode. Much experimental work has been done to come closer to optimizing the system with the intention of going to the commercial market.

Several media applied on the thumb for extracting the fingerprint have been discussed; the good and bad qualities are mentioned. It is probable that the best medium has yet to be found. We know the characteristics of the perfect medium, that it be dry to avoid the initial spike, thin for easy application, and sticky for good contact with the prism. We are confident of the ability of the apparatus to detect fingerprints reliably but it is another matter to believe that it is fool-proof from fraud or practical enough now to be used in the commercial market. A wide statistical study must be done in order to determine the effectiveness of this system.

BIBLIOGRAPHY

1. Max Born and Emil Wolf, "Principles of Optics" (Pergamon Press, 1980).
2. Joseph W. Goodman, "Introduction to Fourier Optics," (McGraw-Hill Inc., 1968).
3. A. B. Vander Lugt, "Signal Detection by Complex Spatial Filtering," Radar Lab., Rept. No. 4594-22-T, Institute of Science and Technology, the University of Michigan, Ann Arbor (1963).
4. A. B. Vander Lugt, "Signal Detection by Complex Spatial Filtering," IEEE Transform Information Theory, IT-10:2(1964).
5. W. Thomas Cathey, "Optical Information Processing and Holography" (John Wiley & Sons, p204, 1974).
6. Henry J. Caulfield and Dean R. Perkins, "Fingerprint Identification Apparatus," United States Patent, 3716301 (1973).

APPENDIX

PARTS LIST:

Transparency system

He-Ne laser: 20 mW, Spectra Physics Inc.
Shutter: Newport Research Corporation (NRC)
Beamsplitter: Model 930-63, NRC
Microscope objective: 20X, 0.40, Edmund Scientific
Right Angle Prism: 1.5"x 1.5"X 1.5", Edmund Scientific
Lens L₁: f=370mm, d=70mm, SROL
Lens L₂: f=370mm, d=70mm, SROL
Lens L₃: Model 32495, f=50mm, d=30mm, Edmund Scientific Scientific
Thermoplastic unit: HC300, NRC
Detector: laser diode array detector, EG&G

Real-time System

Laser Diode: TOLD9520, 635nm, 3mW, Toshiba
Laser diode power supply: 6235A, Hewlett-Packard
Right Angle Prism: 1.5"x 1.5"X 1.5", Edmund Scientific
Lens L₁: Model 32926, f=400mm, d=40mm, Edmund Scientific
Lens L₂: Model 32390, f=100mm, d=38mm, Edmund Scientific
Lens L₃: Model 32495, f=50mm, d=30mm, Edmund Scientific
Right Angle Prism: 1.5"x 1.5"X 1.5", Edmund Scientific
Microscope objective: 20X, 0.40, Edmund Scientific
Holographic Plate: Kodak 10E75
Detector: laser diode array detector, EG&G